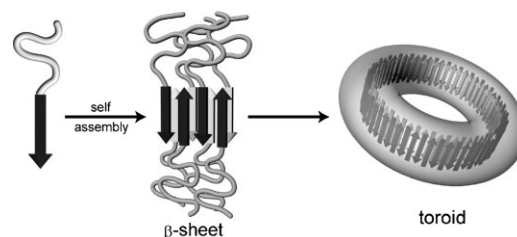


# Toroidal Nanostructures from Self-Assembly of Block Copolypeptides Based on Poly(L-Arginine) and $\beta$ -Sheet Peptide

Yong-beom Lim, Eunji Lee, Myongssoo Lee\*

We demonstrate here that rationally designed block copolypeptides based on poly(L-arginine) and  $\beta$ -sheet peptides can form toroidal nanostructures. In aqueous solution, we found that 1D nanoribbons roll up and connect in an end-to-end fashion under charge-balanced conditions, resulting in the formation of barrel-like toroidal nanostructures. Toroidal diameter was highly uniform (10 nm), indicating that there is a preferred geometrical packing requirement for toroid formation. Our results demonstrate that, when suitably designed,  $\beta$ -sheet nanostructures can be manipulated to form more complex 2D nanostructures. This finding offers new opportunities not only for the fabrication of more sophisticated peptide-based nanobiomaterials, but also for understanding and inhibiting protein misfolding diseases.



## Introduction

Extensive studies on the self-assembly behavior of synthetic amphiphiles have provided structural controls for the preparation of well-defined nanoscopic objects. In contrast to the widespread occurrences of spherical, rod-like, and vesicular structures, only a few examples of toroidal structures have been reported.<sup>[1]</sup> It has been theoretically confirmed that the toroidal structure-dominated regime is very narrow, and that the presence of toroids may be difficult to observe in many micellar systems.<sup>[2]</sup> Formation of toroidal structures has nevertheless been observed in amphiphilic block copolymers,<sup>[1a-c]</sup> surfactants,<sup>[1d,e]</sup> and

rod-coil amphiphiles.<sup>[1f-h]</sup> Cylindrical micelles collapse to form toroids via end-to-end or end-to-body connections when there is a fine balance between the conformational entropy and the end-cap energy.<sup>[1a-e]</sup> A large proportion of the reported toroidal structures has been observed in amphiphiles with charged hydrophilic blocks, where the presence of ionic species (e.g., salts) plays an important role in toroid formation.<sup>[1a,c]</sup>

Self-assembled  $\beta$ -sheet peptides have been the subject of widespread research interest, in part due to their implication in a variety of protein misfolding diseases.<sup>[3]</sup> On the other hand, artificially-designed self-assembled  $\beta$ -sheet peptides have also attracted much attention for their use in the fabrication of novel peptide-based nanobiomaterials.<sup>[4]</sup> The  $\beta$ -sheet fibrils are organized in such a way that each  $\beta$ -strand runs perpendicular to the fibril axis (cross- $\beta$  structure). Regardless of the natural or artificial origin of  $\beta$ -sheet fibrils, the cross- $\beta$  structure has mostly resulted in the formation of one-dimensional (1D) nanostructures. However, it has been found that toroidal structures can be formed as discrete intermediates during the fibrillization of  $\beta$ -amyloid and  $\alpha$ -synuclein.<sup>[5]</sup>

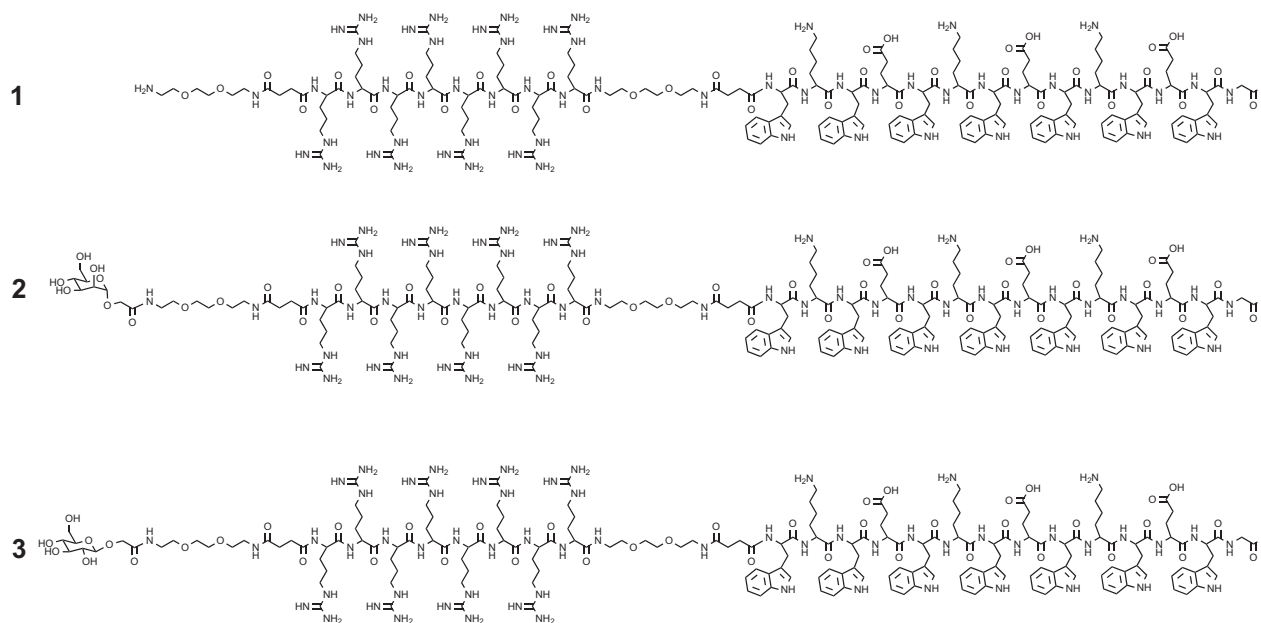
M. Lee, E. Lee

Center for Supramolecular Nano-Assembly and Department of Chemistry, Seoul National University, Seoul 151-742, Korea

Fax: (+82)2-393-6096; E-mail: myongslee@snu.ac.kr

Y.-b. Lim

Translational Research Center for Protein Function Control, Department of Materials Science and Engineering, Yonsei University, Seoul 120-749, Korea



■ Scheme 1. Structures of block copolypeptide building blocks.

Based on these findings, we questioned whether artificial  $\beta$ -sheet peptides can be self-assembled into toroidal structures by adopting molecular structural requirements for toroid formation from synthetic amphiphiles. The design principle for most artificial  $\beta$ -sheet peptides is the alternating placement of charged (or polar) and hydrophobic amino acids.<sup>[6]</sup> This type of arrangement promotes the 1D growth of a cross- $\beta$  structure. However, it has been demonstrated that many peptides having a propensity to form  $\beta$ -sheet nanofibers often interact laterally to form higher order aggregates. To avoid this problem, the coupling of hydrophilic macromolecules such as poly(ethylene glycol) (PEG) on the N- or C-terminus of  $\beta$ -sheet peptides is employed and has been shown to significantly inhibit the formation of higher aggregates and to enhance the solubility of 1D  $\beta$ -sheet structures in aqueous solution.<sup>[7]</sup>

Based on these findings, we envisioned a  $\beta$ -sheet peptide-based block molecule conjugated with a highly charged and flexible hydrophilic block, anticipating that the self-assembly behavior might be similar to that of amphiphiles with charged hydrophilic blocks in aqueous, salt-containing solutions (*vide ante*). With this in mind, we designed a block copolypeptide in which a charged hydrophilic block is attached to a  $\beta$ -sheet forming block. The  $\beta$ -sheet-forming peptide block is composed of alternatively placed hydrophobic (tryptophan), positively charged (lysine), hydrophobic (tryptophan), and negatively charged (glutamic acid) amino acids, which promote  $\beta$ -ribbon formation.<sup>[4a,d]</sup> The hydrophilic block is designed such that multiple positively charged arginine residues are placed between flexible PEG chains (Scheme 1).

## Experimental Part

### Block Copolypeptide Synthesis

The PEG linker, *N*-(Fmoc-8-amino-3,6-dioxaoctyl)succinic acid (Fmoc-PEG<sub>2</sub>-Suc-OH), was purchased from Anaspec, Inc (San Jose, USA). The block copolypeptides were synthesized on pre-loaded Fmoc-Gly-2-chlorotrityl resin using standard Fmoc protocols on Applied Biosystems model 433A peptide synthesizer. For coupling *D*-mannose to the peptide, *N,N'*-diisopropylcarbodiimide (DIC, 15.5  $\mu$ L, 100  $\mu$ mol) was added to a solution of carboxymethyl 2,3,4,6-tetra-*O*-acetyl- $\alpha$ -*D*-mannopyranoside (41 mg, 100  $\mu$ mol) and *N*-hydroxysuccinimide (23 mg, 200  $\mu$ mol) in DCM (1 mL). For coupling *D*-glucose to the peptide, carboxymethyl 2,3,4,6-tetra-*O*-acetyl- $\alpha$ -*D*-glucopyranoside was used. Following overnight reaction at RT, the solvent was evaporated under reduced pressure. The activated acid was dissolved in *N*-methyl-2-pyrrolidone (NMP, 1 mL), mixed with DIPEA (200  $\mu$ mol), and added to the resin-bound peptide (20  $\mu$ mol based on the peptide substitution on the resin). The reaction continued overnight with shaking at room temperature. Following washing the resin, acetyl protecting groups from the carbohydrates were deblocked by the treatment with 10% hydrazine/DMF for 5 h. The resin was washed and dried. The dried resin was treated with cleavage cocktail (TFA: 1,2-ethanedithiol: thioanisole; 95:2.5:2.5) for 3 h, and was triturated with *tert*-butyl methyl ether. The block copolypeptides were purified by reverse-phase HPLC on C<sub>18</sub> column (Vydac, USA) using linear gradient of water to acetonitrile in the presence of 0.1% TFA. The molecular weight was confirmed by MALDI-TOF mass spectrometry. The purity of the building blocks was >95% as determined by analytical HPLC. Concentration was determined spectrophotometrically in water/acetonitrile (1:1) using a molar extinction coefficient of tryptophan (5500 M<sup>-1</sup> · cm<sup>-1</sup>) at 280 nm.

### Circular Dichroism (CD) Spectroscopy and Dynamic Light Scattering (DLS) Experiment

CD spectra were measured using a JASCO model J-810 spectropolarimeter. Typically, peptide ( $20 \times 10^{-6}$  M) was dissolved in appropriate aqueous solution and the spectrum was recorded from 250 to 190 nm using a 0.1 cm path-length cuvette. Scans were repeated five times and averaged. Molar ellipticity was calculated per amino acid residue. DLS experiment was performed at room temperature with ALV/CGS-3 Compact Goniometer System equipped with He-Ne laser operating at 632.8 nm. The scattering angle was  $90^\circ$ . Before measurement, the sample was centrifuged at  $16\,110 \times g$  for 20 min to sediment any dust particles. The size distribution was determined by using a constrained regularization method.<sup>[8]</sup>

### Transmission Electron Microscopy (TEM)

For TEM experiment, 3  $\mu$ L of an aqueous solution of sample was placed onto a carbon-coated copper grid, and 3  $\mu$ L of 2% (w/w) uranyl acetate solution was added for positive staining. The sample was deposited for 1 min, and excess solution was wicked off by filter paper. The specimen was observed with a JEOL-JEM 2010 instrument operating at 120 kV. The cryogenic transmission electron microscopy (TEM) experiments (cryo-TEM) were performed with a thin film of PBS solution of block copolypeptide (5  $\mu$ L) transferred to a lacey supported grid. The thin aqueous films were prepared under controlled temperature and humidity conditions (97–99%) within a custom-built environmental chamber in order to prevent evaporation of water from sample solution. The excess liquid was blotted with filter paper for 2–3 s, and the thin aqueous films were rapidly vitrified by plunging them into liquid ethane (cooled by liquid nitrogen) at its freezing point. The grid was transferred, on a Gatan 626 cryoholder using a cryo-transfer device. After that they were transferred to a JEOL-JEM 2010 TEM instrument. Direct imaging was carried out at a temperature of approximately  $-175^\circ\text{C}$  and with a 120 kV accelerating voltage, while acquiring the images with a SC 1000 CCD camera (Gatan, Inc., USA). The data were analyzed with DigitalMicrograph software.

### Atomic Force Microscopy (AFM)

For AFM, 1  $\mu$ L of the sample in PBS was deposited onto a freshly cleaved mica surface for 1 min, rinsed with water several times, and blown dry with air. The images were obtained in tapping mode with a Nanoscope IIIa instrument (Digital Instruments). AFM scans were taken at setpoint of 0.8–1 V and scanning speed was 1–2 Hz.

### Lectin Agglutination Assay

Fluorescein-labeled Concanavalin A (FAM-Con A) was obtained from Vector laboratories (Burlingame, USA). The Con A was diluted into a concentration of  $0.5 \text{ mg} \cdot \text{mL}^{-1}$  with 10 mM Hepes, 0.15 M NaCl,  $0.1 \times 10^{-3}$  M  $\text{Ca}^{2+}$ ,  $0.01 \times 10^{-3}$  M  $\text{Mn}^{2+}$ , 0.08%  $\text{NaN}_3$ , pH 7.5. For the precipitation assay, 200  $\mu$ L of the Con A solution was mixed with 100  $\mu$ L of block copolypeptide **2** solution in PBS. The mixture incubated for 1 h at room temperature before taking images.

### Results and Discussion

The self-assembly behavior of block copolypeptide **1** was first investigated in phosphate buffered saline (PBS,  $15 \times 10^{-3}$  M potassium phosphate,  $150 \times 10^{-3}$  M NaCl, pH 7.4), a physiological buffer. A circular dichroism (CD) spectrum of block copolypeptide **1** showed characteristic  $\beta$ -sheet structure formation. Zeta-potential ( $\zeta$ ) measurement showed that the  $\beta$ -sheet-mediated self-assembled structures had positive  $\zeta$  potential values ( $+37.5 \pm 6.1$  mV), indicating the formation of the positively charged surface due to arginine guanidinium groups. To investigate the nanostructural morphology of **1**, TEM was performed with negatively stained samples. As can normally be expected in PEG-conjugated  $\beta$ -sheet peptide assemblies, many discrete fibrous  $\beta$ -ribbon structures were formed (Figure 1a). Remarkably, toroidal structures were found to coexist with the  $\beta$ -ribbon structures, although their numbers were small.

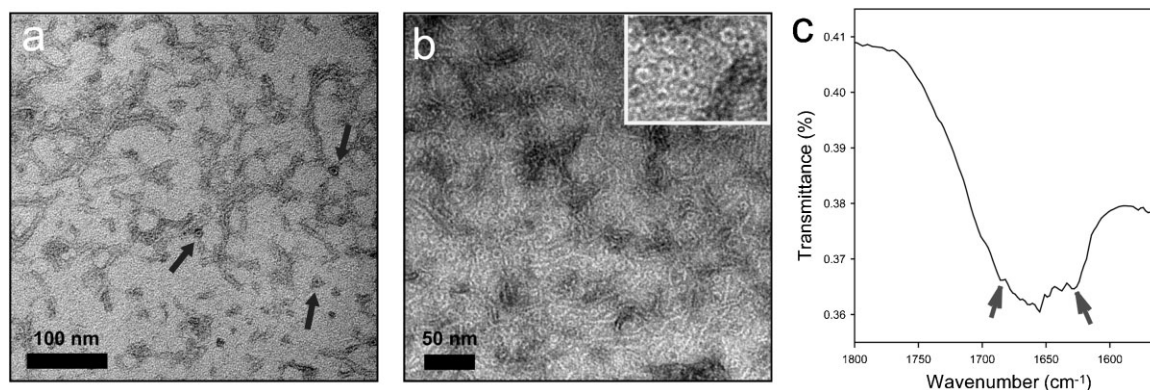


**Figure 1.** a) TEM image of block copolypeptide **1** in PBS. Arrows indicate toroids. b) TEM image of block copolypeptide **2** in PBS. c) FT-IR spectrum of **2**. Arrows indicate bands at  $1684$  and  $1628 \text{ cm}^{-1}$ , which are the characteristics of antiparallel  $\beta$ -sheet conformation. Other amide I bands between  $1684$  and  $1628 \text{ cm}^{-1}$  are likely to be originated from the random-coiled hydrophilic block. The block peptide in PBS solution was cast onto ZnSe window.

To determine whether an increase in volume fraction of hydrophilic blocks further stabilizes the toroidal structure, we designed block copolyptide **2**, in which polar and charge neutral carbohydrate mannose was attached to the N-terminus of block copolyptide **1**. Carbohydrate mannose was chosen with the aim of imparting biological functionality to the nanostructures.<sup>[9]</sup> Indeed, nanostructures formed from block copolyptide **2** exhibit higher populations of toroidal nanostructures than those from block copolyptide **1** (Figure 1b). Further, the toroidal micelles have almost the same cross section (of about 3 nm) as the coexisting  $\beta$ -ribbons, suggesting that toroids are formed through the collapse of  $\beta$ -ribbons.

Toroidal diameter was highly uniform ( $9.8 \pm 0.8$  nm), indicating that there is a preferred geometrical packing for toroid formation. Contrary to the coexistence of a variety of morphologies, such as lariats, Y-junctions, figure eights, and dumbbells in toroid-forming block copolymers,<sup>[1a,b]</sup> only two structures ( $\beta$ -ribbons and toroids) were observed. This finding, together with the uniform toroid sizes, suggests that toroids are likely to form via end-to-end connections of  $\beta$ -ribbons. An infrared (IR) spectrum of **2** shows that  $\beta$ -strands assemble in an antiparallel arrangement (Figure 1c). The fully extended and rigid  $\beta$ -strands are likely to be oriented perpendicular to the toroid plane in order to be accommodated into a severely angled toroidal structure, resulting in the formation of  $\beta$ -barrel structures (Figure 2). Similar results were obtained with block copolyptide **3**, in which the carbohydrate glucose is attached, implying that a small variation in structure from block copolyptide **2** is tolerable for toroid formation. In addition, the self-

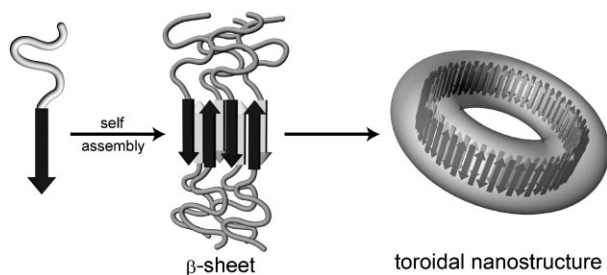


**Figure 2.** Toroidal nanostructure formation from block copolypeptides based on poly(L-arginine) and  $\beta$ -sheet peptide.

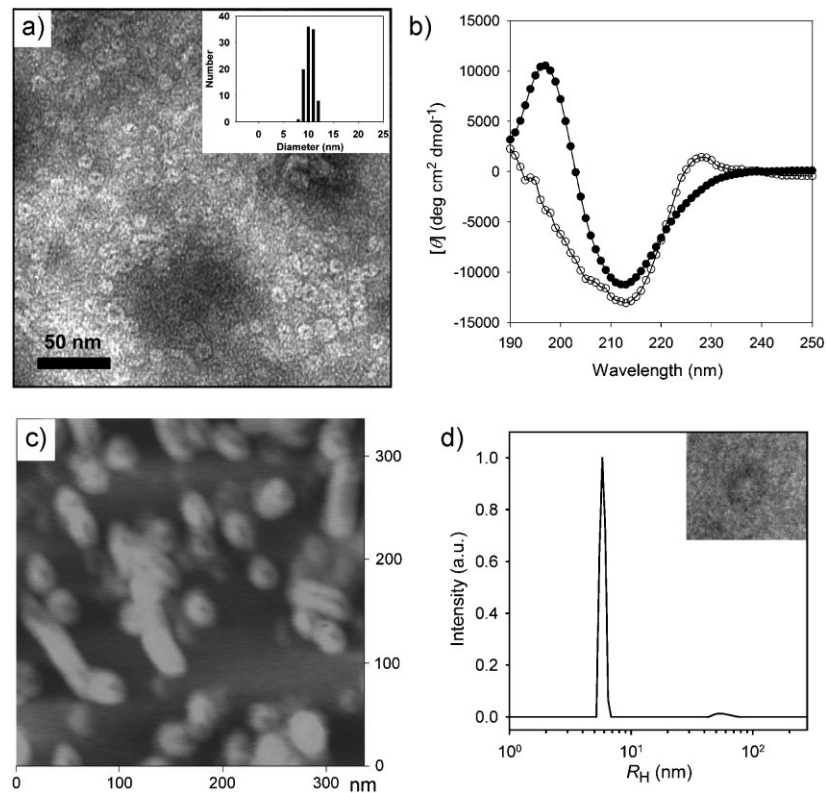


**Figure 3.** a) TEM image obtained after slow addition of salt. PBS was slowly added to block copolyptide **2** dissolved in water. Inset: size distribution of toroids. b) CD spectra of block copolyptide **2** in water (open circle) and PBS (closed circle). c) AFM image of **2**. d) DLS analysis of **2**. Inset: cryo-TEM image.

assembly behavior was similar regardless of peptide building block concentrations. A comprehensive and detailed study on how the block copolyptide structure affects toroid formation is the subject of ongoing research.

We next investigated the influence of salt on toroid formation. Only very small populations of toroids in block copolyptide **2** were observed in pure water, suggesting that salt presence is important for toroid formation. Substitution of sodium chloride with potassium fluoride in the preparation of PBS had no adverse influence on toroid formation. Next, we inquired whether toroid formation is independent of pH or phosphate ions present in PBS. The results showed that presence of salt is a sufficient condition for toroidal structure formation. Finally, it was found that the population of toroidal structures could be dramatically increased by slowly stabilizing the  $\beta$ -sheet structure. This condition could be achieved by very slowly adding salt-containing solution to the block copolyptide solution in water. As shown in Figure 3a, the slow addition of PBS to block copolyptide **2** solution resulted in the formation of toroidal structures as the predominant species, indicating that stringent and highly regulated conditions are required to allow for the connection of both ends of the  $\beta$ -ribbons.



Furthermore, a CD spectrum of **2** shows that  $\beta$ -sheet structures are better stabilized in a salt-containing solution than they are in pure water (Figure 3b).<sup>[4a]</sup> Screening of charged arginine residues and the following decrease in electrostatic repulsion among hydrophilic blocks are likely responsible for the salt-induced toroid formation.<sup>[1c]</sup> It should be noted that the overall shape and intensity of CD spectra were similar irrespective of the salt addition rate. This result implies that  $\beta$ -sheet formation efficiency is not affected by the salt addition rate. The formation of a dominant population of toroids was further confirmed through atomic force microscopy (AFM), as shown in Figure 3c.

To confirm that toroids are not formed during a solvent evaporation process or by staining reagent while preparing TEM samples on the grid, cryo-TEM, and dynamic light scattering (DLS) experiments were performed. The inset in Figure 3d shows dark toroidal objects of block copolypeptide **2** against the vitrified solution background, demonstrating that the toroids are formed in bulk solution. DLS experiments further corroborated this, as the DLS data showed a bimodal distribution of hydrodynamic radius ( $R_H$ ) centered at 5.8 and 53.9 nm (Figure 3d). As the radius of the toroid was found to be 4.9 nm from TEM data, the predominant smaller aggregates should correspond to toroidal structures, while the small population of larger aggregates corresponded to  $\beta$ -ribbons. The small difference in the aggregate sizes between the DLS and TEM data (5.8 versus 4.9 nm) is likely due to the fact that the hydrophilic block is hydrated and extended under DLS solution conditions, whereas the sample is in the dried state during TEM investigation.

Since the toroidal nanostructures of **2** and **3** are covered with multiple carbohydrates, the toroidal nanostructures can act as useful multivalent scaffolds<sup>[9,10]</sup> for carbohydrates. In order to determine whether multiple copies of carbohydrates in the toroidal nanostructures of **2** and **3** can enhance the affinity of carbohydrate-protein interactions via the "glycosidic cluster effect," we performed a lectin agglutination assay.<sup>[11]</sup> Upon addition of lectin (fluorescein-labeled Con A) to a solution of **2**, the solution became turbid due to aggregate formation and the subsequent aggregate precipitation over time, which indicates multivalent interactions between the toroids and the lectins (Figure 4). These results imply that the carbohydrate-coated toroids can be used as new multivalent ligands with unique circular nanogeometry.

## Conclusion

In conclusion, we have shown that  $\beta$ -sheet-forming peptides can form toroidal nanostructures in solution when they are attached to highly charged blocks of the

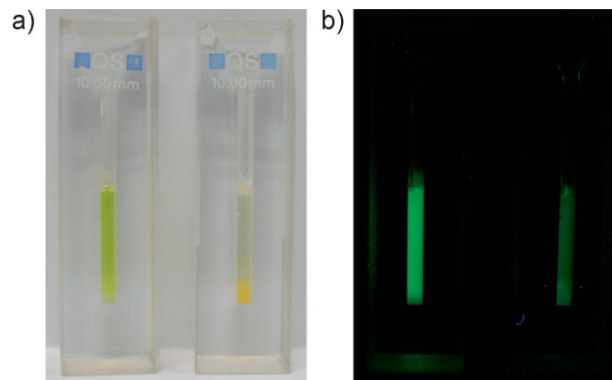


**Figure 4.** Multivalent interactions between toroids and lectins. Lectin agglutination assay. a) Image taken at ambient light. b) Fluorescence image taken after UV irradiation. Left; FAM-Con A alone, right; Con A plus block peptide **2** nanostructures.

appropriate molecular structure. This finding offers new opportunities for the fabrication of more complex and sophisticated peptide-based materials with enhanced properties. An in-depth study of the kinetics and thermodynamics of toroid assembly, structural requirements, and the morphological stabilities should be the subjects of further investigation. These issues are important not only for developing functional  $\beta$ -sheet peptide nanobiomaterials, but also for understanding and inhibiting protein misfolding diseases such as amyloid fibrogenesis.

**Acknowledgements:** M. L. acknowledges a grant from the National Creative Research Initiative Program of the *National Research Foundation (NRF)* of Korea and *U.S. Air Force Office of Scientific Research (FA 2386-10-1-4087)*. Y.-b. L. thanks the *NRF* for support through the *Future-based Technology Development Program (Nano Fields; 2010-0019102)*, the *Basic Science Research Program (2010-0015374 and 2010-0016145)*, and the *Translational Research Center for Protein Function Control, Yonsei University (2010-0001933)*.

Received: August 15, 2010; Published online: November 15, 2010;  
DOI: 10.1002/marc.201000512

**Keywords:** biomaterials; peptides; self-assembly;  $\beta$ -sheets; toroids

- [1] [1a] D. J. Pochan, Z. Chen, H. Cui, K. Hales, K. Qi, K. L. Wooley, *Science* **2004**, *306*, 94; [1b] S. Jain, F. S. Bates, *Science* **2003**, *300*, 460; [1c] S. Förster, N. Hermsdorf, W. Leube, H. Schnablegger, M. Regenbrecht, S. Akari, P. Linder, C. Böttcher, *J. Phys. Chem. B* **1999**, *103*, 6657; [1d] A. Bernheim-Groswasser, R. Zana, Y. Talmon, *J. Phys. Chem. B* **2000**, *104*, 4005; [1e] M. In, O. Aguerre-Chariol, R. Zana, *J. Phys. Chem. B* **1999**, *103*,

- 7747; [1f] W.-Y. Yang, J.-H. Ahn, Y.-S. Yoo, N.-K. Oh, M. Lee, *Nat. Mater.* **2005**, *4*, 399; [1g] J.-K. Kim, E. Lee, Z. Huang, M. Lee, *J. Am. Chem. Soc.* **2006**, *128*, 14022; [1h] E. Lee, J.-K. Kim, M. Lee, *J. Am. Chem. Soc.* **2009**, *131*, 18242.
- [2] P. van der Schoot, J. P. Wittmer, *Macromol. Theory Simul.* **1999**, *8*, 428.
- [3] [3a] C. M. Dobson, *Nature* **2003**, *426*, 884; [3b] I. W. Hamley, *Angew. Chem., Int. Ed.* **2007**, *46*, 8128; [3c] R. Mimna, M.-S. Camus, A. Schmid, G. Tuchscherer, H. A. Lashuel, M. Mutter, *Angew. Chem., Int. Ed.* **2007**, *46*, 2681.
- [4] [4a] Y.-b. Lim, E. Lee, M. Lee, *Angew. Chem., Int. Ed.* **2007**, *46*, 3475; [4b] Y.-b. Lim, S. Park, E. Lee, H. Jeong, J.-H. Ryu, M. S. Lee, M. Lee, *Biomacromolecules* **2007**, *8*, 1404; [4c] H. G. Börner, H. Schlaad, *Soft Matter* **2007**, *3*, 394; [4d] D. M. Marini, W. Hwang, D. A. Lauffenburger, S. Zhang, R. D. Kamm, *Nano Lett.* **2002**, *2*, 295; [4e] C. W. G. Fishwick, A. J. Beevers, L. M. Carrick, C. D. Whitehouse, A. Aggeli, N. Boden, *Nano Lett.* **2003**, *3*, 1475; [4f] K. Matsuura, K. Murasato, N. Kimizuka, *J. Am. Chem. Soc.* **2005**, *127*, 10148; [4g] G. T. Dolphil, P. Dumy, J. Garcia, *Angew. Chem., Int. Ed.* **2006**, *45*, 2699; [4h] Y.-b. Lim, K.-S. Moon, M. Lee, *Chem. Soc. Rev.* **2009**, *38*, 925; [4i] Y.-b. Lim, K.-S. Moon, M. Lee, *Angew. Chem., Int. Ed.* **2009**, *48*, 1601.
- [5] H. A. Lashuel, D. Hartley, B. M. Petre, T. Walz, P. T. Lansbury, Jr, *Nature* **2002**, *418*, 291.
- [6] Y.-b. Lim, M. Lee, *J. Mater. Chem.* **2008**, *18*, 723.
- [7] T. S. Burkoth, T. L. S. Benzinger, D. N. M. Jones, K. Hallenga, S. C. Meredith, D. G. Lynn, *J. Am. Chem. Soc.* **1998**, *120*, 7655.
- [8] T. G. Braginskaya, P. D. Dobitchin, M. A. Ivanova, V. V. Klyubin, A. V. Lomakin, V. A. Noskin, G. E. Shmelev, S. P. Tolpina, *Phys. Scr.* **1983**, *28*, 73.
- [9] [9a] Y.-b. Lim, M. Lee, *Org. Biomol. Chem.* **2007**, *5*, 401; [9b] Y.-b. Lim, S. Park, E. Lee, J.-H. Ryu, Y.-R. Yoon, T.-H. Kim, M. Lee, *Chem. Asian J.* **2007**, *2*, 1363; [9c] J.-H. Ryu, E. Lee, Y.-b. Lim, M. Lee, *J. Am. Chem. Soc.* **2007**, *129*, 4808.
- [10] L. Gu, T. Elkin, X. Jiang, H. Li, Y. Lin, L. Qu, T.-R. J. Tzeng, R. Joseph, Y.-P. Sun, *Chem. Commun.* **2005**, 874.
- [11] J. E. Gestwicki, L. E. Strong, C. W. Cairo, F. J. Boehm, L. L. Kiessling, *Chem. Biol.* **2002**, *9*, 163.